Flavokawain B inhibits growth of human squamous carcinoma cells: involvement of apoptosis and cell cycle dysregulation *in vitro* and *in vivo*

Elong Lin[a], Wen-Hsin Lin[b], Sheng-Yang Wang[c], Chih-Sheng Chen[h], Jiuun-Wang Liao[d], Hsueh-Wei Chang[e], Ssu-Ching Chen[f], Kai-Yuan Lin[g], Lai Wang[h], Hsin-Ling Yang[h,*], You-Cheng Hseu[i,*]

[a]*Department of Food Science and Technology, Central Taiwan University, Taichung, Taiwan*
[b]*School of Pharmacy, China Medical University, Taichung, Taiwan*
[c]*Department of Forestry, National Chung-Hsing University, Taichung, Taiwan*
[d]*Graduate Institute of Veterinary Pathology, National Chung-Hsing University, Taichung, Taiwan*
[e]*Department of Biomedical Science and Environmental Biology, Graduate Institute of Natural Products, College of Pharmacy, Center of Excellence for Environmental Medicine, Kaohsiung Medical University, Kaohsiung, Taiwan*
[f]*Department of Life Sciences, National Central University, Chung-Li, Taiwan*
[g]*Department of Medical Research, Chi-Mei Medical Center, Tainan, Taiwan*
[h]*Institute of Nutrition, China Medical University, Taichung, Taiwan*
[i]*Department of Cosmeceutics, China Medical University, Taichung, Taiwan*

Abstract

Flavokawain B is a natural chalcone isolated from the rhizomes of *Alpenia pricei* Hayata. In the present study, we have investigated the antiproliferative and apoptotic effect of flavokawain B (5–20 μg/ml; 17.6–70.4 μM) against human squamous carcinoma (KB) cells. Exposure of KB cells with flavokawain B resulted in apoptosis, evidenced by loss of cell viability, profound morphological changes, genomic DNA fragmentation and sub-G1 phase accumulation. Apoptosis induced by flavokawain B results in activation of caspase-9, -3 and -8, cleavage of PARP and Bid in KB cells. Flavokawain B also down-regulate Bcl-2 with concomitant increase in Bax level, which resulted in release of cytochrome *c*. Taken together, the induction of apoptosis by flavokawain B involved in both death receptor and mitochondrial pathway. We also observed that flavokawain B caused the G2/M phase arrest that was mediated through reductions in the levels of cyclin A, cyclin B1, Cdc2 and Cdc25C and increases in p21/WAF1, Wee1 and p53 levels. Moreover, flavokawain B significantly inhibits matrix metalloproteinase-9 and urokinase plasminogen activator expression, whereas tissue inhibitor of matrix metalloproteinase-1 and plasminogen activator inhibitor-1 were increased, which are playing critical role in tumor metastasis. In addition, flavokawain B treatment significantly inhibited *in vivo* growth of human KB cell-derived tumor xenografts in nude mice, which is evidenced by augmentation of apoptotic DNA fragmentation, as detected by *in situ* terminal deoxynucleotidyl transferase-meditated dUTP nick end-labeling staining. The induction of cell cycle arrest and apoptosis by flavokawain B may provide a pivotal mechanism for its cancer chemopreventive action.
© 2011 Published by Elsevier Inc.

Keywords: Flavokawain B; Cell cycle arrest; Apoptosis; KB cells

1. Introduction

The rhizomes of Zingiberaceae including ginger, turmeric and cardamon plants are widely used as spices in Asian countries, eaten raw, cooked as vegetables or used as flavoring [1]. *Alpinia* plants (shell gingers, family Zingiberaceae) have been shown by several previous studies to have various biological activities, including, antioxidant, anti-inflammatory, anticancer, immunostimulating, hepatoprotective and antinociceptive activities [2,3]. *A. pricei* Hayata is a perennial rhizomatous plant indigenous to Taiwan. It has various traditional and commercial uses, such as use of the leaves to make traditional zongzi (glutinous rice dumplings) in Taiwan and use of the aromatic rhizomes as a folk medicine for dispelling abdominal distension and enhancing stomach secretion and peristalsis [4]. In earlier studies, we demonstrated that ethanol (70%) extracts of *A. pricei* exhibit antitumor effects by induction of cell cycle arrest/apoptosis in human squamous carcinoma KB cells [2,5]. However, the phytochemistry and bioactivity of *A. pricei* extracts have not yet been elucidated.

Chemoprevention, which refers to the administration of agents to prevent initiation and promotion of events associated with carcinogenesis, is being increasingly considered an effective approach for the management of neoplasms. Many studies investigating the use of cell cycle inhibitors and apoptosis-inducing agents for the management of

* Corresponding authors. Hsin-Ling Yang is to be contacted at Institute of Nutrition, China Medical University, Taichung 40402, Taiwan; You-Cheng Hseu, Department of Cosmeceutics, China Medical University, Taichung 40402, Taiwan. Tel.: +886 4 22053366x5308; fax: +886 4 22078083.
E-mail addresses: hlyang@mail.cmu.edu.tw (H. L. Yang), ychseu@mail.cmu.edu.tw (Y. C. Hseu).

cancer have shown associations between abnormal cell cycle regulation and apoptosis and cancer [6]. Eukaryotic cell cycle progression involves the sequential activation of cyclin-dependent kinases (CDKs), which is dependent on association with cyclins [7]. Progression through the mammalian mitotic cycle is controlled by multiple holoenzymes, including a catalytic CDK and a cyclin regulatory subunit [7]. These cyclin–CDK complexes are activated at specific intervals during the cell cycle but can be induced and regulated by exogenous factors. Apoptosis is characterized by a number of well-defined features, including cellular morphological changes, chromatin condensation, internucleosomal DNA cleavage and the activation of a family of cysteine-aspartic acid proteases (caspases) [8]. Thus, agents that alter regulation of cell cycle machinery, resulting in arrest in different phases, thereby reducing growth and proliferation of, and even inducing apoptosis in, cancerous cells, may be useful in cancer chemoprevention.

Found abundantly in edible plants, chalcones (1,3-diaryl-2-propen-1-ones) are important biological compounds and are precursors in the biosynthesis of flavonoids and isoflavonoids. Chalcones have been reported to possess many useful properties, including anti-inflammatory, antimicrobial, antifungal, antioxidant, cytotoxic, anti-tumor and anticancer activities [9,10]. It has bee shown that flavokawains, chalcone derivatives in kava extracts as used by South Pacific Islanders for thousands of years, are novel apoptosis inducers and anticarcinogenic agents [11]. Studies have identified that flavokawain A from extracts of kava (*Piper methylsticum*) roots can induce apoptosis and cell cycle arrest in the invasive bladder cancer cell line T24 and that flavokawains B and C, also from kava extract, have strong antiproliferative effects against several cancer cell lines (RT4, T24 and EJ cells) [11]. The rootstock of kava is commonly used to prepare a beverage for ceremonial activities by the native Pacific Islanders. An epidemiologic study found that cancer incidence in the three highest kava-drinking countries — Vanuatu, Fiji and Western Samoa — was one quarter to one third of those in non-kava-drinking countries, such as New Zealand (Maoris) and the United States (Hawaii and Los Angeles) [12]. These findings should encourage the development of more potent chalcone derivatives for both prevention and treatment of cancer, as well as epidemiologic studies of the relationship between flavokawain consumption and cancer. Here, we investigate the anticancer effects of flavokawain B (5–20 μg/ml; 17.6–70.4 μM), a chalcone purified from ethanol (70%) extracts of *A. pricei* rhizomes, in terms of tumor regression using both *in vitro* cell culture and *in vivo* athymic nude mice models of KB cells. The levels of cell cycle/apoptosis/metastatic control and related molecules were assayed to determine the flavokawain B anticancer mechanism.

2. Materials and methods

2.1. Reagents

Dulbecco's modified Eagle's medium (DMEM) contained the following: fetal bovine serum (FBS), glutamine and penicillin/streptomycin/neomycin (GIBCO BRL, Grand Island, NY, USA); antibodies against cytochrome *c*, caspase-3, caspase-8, caspase-9, Bcl-2, Bax, Fas, Fas ligand (FasL), cyclin B1, Cdc2, p21/WAF1, Wee1, p53, matrix metalloproteinase-9 (MMP-9), urokinase plasminogen activator (u-PA), tissue inhibitor of matrix metalloproteinase-1 (TIMP-1) and plasminogen activator inhibitor-1 (PAI-1) (Santa Cruz Biotechnology Inc., Heidelberg, Germany); PARP rabbit polyclonal antibody (Upstate Biotechnology, Lake Placid, NY, USA); antibody against β-actin (Sigma Chemical Co., St. Louis, MO, USA) and antibodies against Bid, cyclin A and Cdc25C (Cell Signaling Technology Inc., Danvers, MA), which were obtained from their respective suppliers. All other chemicals were of the highest grade commercially available and supplied either by Merck (Darmstadt, Germany) or Sigma.

2.2. Identification and quantification of flavokawain B in A. pricei extracts

Air-dried roots (2 kg) of *A. pricei* were extracted with 10 L of 70% (vol/vol) ethanol at room temperature as previously described [2]. We further characterized the main composition of *A. pricei* extracts using chromatography followed by spectral analysis. *A. pricei* extracts were separated by semipreparative high-performance liquid chromatography. A Luna silica column (250×10 mm, Phenomenex Co.) was used with two solvent systems: A, H_2O, and B, acetonitrile. The gradient elution profile was as follows: 0–3 min, 80% A to B; 3–60 min, 80–0% A to B (linear gradient) and 60–80 min 0% A to B. The flow rate was 2.5 ml/min, and the detector wavelength was set at 280 nm. The three major compounds in the *A. pricei* extracts were obtained at retention times of (1) 32.5 min, (2) 37.0 min and (3) 46.7 min. The structures of compounds 1–3 were determined by spectroscopic analysis. The UV spectra of these compounds were recorded with a Jasco V-550 spectrometer, and the infrared spectra were obtained with a Bio-Rad FTS-40 spectrophotometer. Electron-impact mass spectrometry and high-resolution electron-impact mass spectrometry data were collected with a Finnigan MAT-958 mass spectrometer. The nuclear magnetic resonance (NMR) spectra were recorded with Bruker Avance 500 and 300 MHz FT-NMR spectrometers, at 500 MHz (^{1}H) and 75 MHz (^{13}C). According to the mass and NMR analysis, compounds 1–3 were identified as: (1) desmethoxyyangonin, (2) cardamonin and (3) flavokawain B [11]. The standard calibration curves (peak area vs. concentrations) of compounds 1–3 ranged from 5 to 100 μg/ml. The linear regression equations were

desmethoxyyangonin	$y=13,134x+13, 147$
cardamonin	$y=25,853x+2128.6$
flavokawain B	$y=11,211x+14, 573$

Each of these equations showed good linearity ($R^2=0.9995–0.9998$). According to the results of high-performance liquid chromatography analysis, the amounts of the compounds desmethoxyyangonin, cardamonin and flavokawain B in *A. pricei* extracts were 1.1%, 8.9% and 5.7%, respectively. Stock solutions of desmethoxyyangonin (1.1 mg), cardamonin (1.2 mg) and flavokawain B (10 mg) were prepared in 100% dimethyl sulfoxide (DMSO) at 25°C, then stored at −20°C.

2.3. Cell culture and assessment of cell viability

The human squamous carcinoma cell line KB (*HeLa* derivative) and the human gingival fibroblast (HGF) cell line HGF were obtained from the American Type Culture Collection (Rockville, MD, USA). The KB cell line was used by the National Cancer Institute for some of the earliest *in vitro* anticancer drug-screening work [13]. KB cells were once thought to be derived from an oral cancer, but in fact, they were derived from a glandular cancer of the cervix [13]. KB and HGF cells were grown in a humidified incubator (5% CO_2 in air at 37°C) in DMEM supplemented with 10% heat-inactivated FBS, 2 mol/l glutamine, 1% penicillin, 1% streptomycin and 1% neomycin. Cells were seeded in 6- or 12-well plates before the addition of flavokawain B. Cultures were harvested, and cell number was determined by counting cell suspensions using a hemocytometer. Cell viability ($3.0×10^5$ cells/12 wells) and growth ($1.0×10^5$ cells/6 wells) were assayed before and after treatment with flavokawain B using trypan blue exclusion and phase contrast microscopy.

2.4. Terminal deoxynucleotidyl transferase-mediated dUTP nick end-labeling assay for DNA apoptotic fragmentation

DNA fragmentation was detected using terminal deoxynucleotidyl transferase-mediated dUTP nick end-labeling (TUNEL) with the Klenow FrgEL DNA fragmentation detection kit (Calbiochem, San Diego, CA, USA). Briefly, KB cells ($5×10^5$ cells/6 wells) were harvested, fixed with 4% formaldehyde and applied to glass slides. Fixed cells were permeabilized with 20 μg/ml of protease K in TBS and endogenous peroxidase was inactivated by 3% H_2O_2 in methanol. Apoptosis was detected by labeling 3′-OH ends of fragmented DNA with biotin–dNTP using Klenow at 37°C for 1.5 h. Slides were then incubated with streptavidin–horseradish peroxidase conjugate for 30 min, followed by incubation with 3,3′-diaminobenzidine and H_2O_2 for 10 min. Apoptotic cells were identified by their dark brown nuclei as seen under a light microscope.

2.5. Flow cytometric analysis

Cellular DNA content was determined by flow cytometric analysis of propidium iodide (PI)-labeled cells. After plates of KB cells ($1×10^6$ cells/ml) were grown to semiconfluence, cell growth was arrested by washing plates with growth media supplemented with 1% FBS. Growth arrest was maintained for 24 h. The cell cycle synchronized cells were then washed with phosphate-buffered saline (PBS) and restimulated to enter the G1 phase together by addition of growth media containing flavokawain B, without FBS. After treatment with flavokawain B (5–20 μg/ml for 24, 48 and 72 h), cells were collected by trypsinization and fixed in 70% ethanol at −20°C overnight. Cells were suspended in PBS containing 1% Triton X-100, 0.5 mg/ml RNase and 4 μg/ml PI at 37°C for 30 min. A FACSCalibur flow cytometer (Becton Dickinson, San Jose, CA, USA) equipped with a single argon ion laser (488 nm) was used for flow cytometric analysis. Forward and right-angle light scattering, correlated with cell size and cytoplasmic complexity, respectively, were used to establish size gates and exclude cellular debris from the analysis. The DNA content of 10,000 cells/analysis was monitored using the FACSCalibur system. Apoptotic nuclei were identified as a subploid DNA peak and were distinguished from cell debris on the basis of forward light scattering and PI fluorescence. Cell cycle profiles were analyzed with ModFit software (Verity Software House, Topsham, ME, USA).

2.6. Measurement of reactive oxygen species generation

Production of intracellular reactive oxygen species (ROS) was detected by fluorescence microscopy or flow cytometry using 2′,7′-dihydrofluorescein-diacetate (DCFH-DA). Cells (5×10^5 cells/6 wells) were cultured in DMEM supplemented with 10% heat-inactivated FBS, with renewal of the culture medium when the cells reached 80% confluence. Samples were then incubated with 10 μmol/l DCFH-DA in culture medium at 37°C for 30 min. During loading, the acetate groups on DCFH-DA were removed by intracellular esterase, trapping the probe inside the KB cells. After loading, cells were washed with warm PBS buffer. Production of ROS species can be measured by changes in fluorescence due to intracellular production of dichlorofluorescein (DCF) caused by oxidation of DCFH. Intracellular ROS, as indicated by DCF fluorescence, was measured with a fluorescence microscope (Olympus 1X 71) or a flow cytometer (FACSCalibur).

2.7. Analysis of mitochondrial membrane potential

The loss of mitochondrial membrane potential was assessed by flow cytometry. Cells (5×10^5 cells/6 wells) were harvested and washed twice, suspended in 500 μl of DiOC6 (20 μmol/l) and incubated at 37°C for 30 min. The excitation wavelength was 488 nm, with monitoring at 530 nm (DiOC6). Cell percentages were calculated with ModFit software.

2.8. Western blotting

KB cells (3.0×10^6 cells/100-mm dish) were detached, washed once in cold PBS and then suspended in 100 μl lysis buffer (10 mmol/l Tris–HCl, pH 8, 0.32 mol/l sucrose, 1% Triton X-100, 5 mmol/l EDTA, 2 mmol/l DTT, 1 mmol/l PMSF). Suspensions were kept on ice for 20 min, then centrifuged at $13,000 \times g$ for 20 min at 4°C. Total protein content was determined with the Bio-Rad protein assay reagent, using BSA as the standard. Protein extracts were reconstituted in sample buffer [0.062 mol/l Tris–HCl, 2% sodium dodecyl sulfate (SDS), 10% glycerol, 5% β-mercaptoethanol], and the mixture was boiled for 5 min. Equal amounts (50 μg) of denatured protein samples were loaded into each lane, separated by SDS–polyacrylamide gel electrophoresis (PAGE) on an 8%–15% polyacrylamide gradient and then transferred to polyvinylidene difluoride membranes overnight. Membranes were blocked with 0.1% Tween-20 in PBS containing 5% (wt/vol) nonfat dried milk for 20 min at room temperature, incubated with primary antibodies for 2 h, then incubated with either horseradish peroxidase-conjugated goat antirabbit or antimouse antibodies for 2 h before being developed using the SuperSignal ULTRA chemiluminescence substrate (Pierce, Rockford, IL, USA). Band intensities were quantified by densitometry, with the absorbance of the mixture at 540 nm determined using an enzyme-linked immunosorbent assay plate reader. Western blot analysis, with antibodies against cytochrome c, caspase-3, caspase-8, caspase-9, PARP, Bcl-2, Bax, Fas, FasL, Bid, cyclin A, cyclin B1, Cdc2, Cdc25C, p21/WAF1, Wee1, p53, MMP-9, u-PA, TIMP-1 and PAI-1, was done as previously described [2].

2.9. Determination of MMP-9 activity by zymography

MMP-9 activity in the medium was measured using a gelatin zymography protease assay [14]. Briefly, an appropriate volume (adjusted by vital cell number) of medium was collected and prepared in SDS sample buffer without boiling or reduction and then subjected to SDS-PAGE (8% polyacrylamide, 0.1% gelatin). Following electrophoresis, gels were washed with 2.5% Triton X-100, incubated in reaction buffer (40 mmol/l Tris–HCl, pH 8.0; 10 mmol/l CaCl$_2$; 0.01% NaN$_3$) at 37°C for 24 h and then stained with CBB R-250.

2.10. Animals

Female athymic nude mice (BALB/c-nu), 5–7 weeks of age, were purchased from GlycoNex, Inc., Taiwan, and were maintained in caged housing in a specifically designed pathogen-free isolation facility with a 12/12-h light–dark cycle; mice were provided rodent chow and water ad libitum. All experiments were conducted in accordance with the guidelines of the China Medical University Animal Ethics Research Board.

2.11. Tumor cell inoculation

KB cells were grown in DMEM medium supplemented with 10% heat-inactivated FBS, 2 mmol/l glutamine and 1% penicillin–streptomycin–neomycin in a humidified incubator (5% CO$_2$ in air at 37°C). Experiments were performed using cells from fewer than 20 passages. Cells (1×10^6) were mixed in a 200-μl atrix gel including growth factors and then injected subcutaneously on the right-hind flank. Tumor volume, as determined by caliper measurements of tumor length, width, and depth, were calculated using the formula: length×width^2×0.5236, every 3 days [15]. In this study, the three pretested mouse ($n=1$) received intraperitoneal injections of flavokawain B at doses of 0, 0.35 and 0.75 mg/kg. Tumor growth and volume significantly decreased with a flavokawain B dose of 0.75 mg/kg, which suggested that this dose should be used in xenografted nude mice. Therefore, two groups received intraperitoneal injections of flavokawain B (0.2 ml/mouse) dissolved in 0.1% DMSO buffer at a dose of 0.75 mg/kg every 2 days, while the control group received daily injections of vehicle only. Following 27 days of treatment, the mice were photographed and killed. Tumors were removed before fixing in 4% paraformaldehyde, sectioning, and staining with hematoxylin–eosin for light microscopy. Samples tissue from each tumor tissue was immediately frozen, and the rest were fixed in 10% neutral-buffered formalin and embedded in paraffin. To monitor drug toxicity, the body weight of each animal was measured every 3 days. In addition, a pathologist examined the mouse organs, including the liver, lungs and kidneys.

2.12. In situ apoptosis detection

Apoptotic cell death in deparaffinized tissue sections was detected using TUNEL with the Klenow DNA fragmentation detection kit (Calbiochem) [16]. Briefly, sections were permeabilized with 20 μg/ml protease K in TBS and endogenous peroxidase was inactivated by 3% H$_2$O$_2$ in methanol. Apoptosis was detected by labeling 3′-OH ends of fragmented DNA with biotin–dNTP using Klenow at 37°C for 1.5 h. Slides were then incubated with streptavidin–horseradish peroxidase conjugate, followed by incubation with 3,3′-diaminobenzidine and H$_2$O$_2$. Apoptotic cells were identified by the dark brown nuclei observed under light microscopy.

2.13. Statistics

In vitro results are presented as mean±standard deviation (mean±S.D.). For in vivo experiments, mean data values are presented with standard error (mean±S.E.). All study data were analyzed using analysis of variance, followed by Dunnett's test for pairwise comparison. Statistical significance was defined as $P<.05$ for all tests.

3. Results

In this study, the human squamous carcinoma cell line KB was used to investigate the capability of flavokawain B (5–20 μg/ml), a chalcone purified from ethanol (70%) extracts of A. pricei rhizomes, to induce cell cycle arrest and apoptosis, and to elucidate the molecular mechanisms involved.

3.1. Effects of desmethoxyyangonin, cardamonin and flavokawain B on KB cell death

To investigate the effects of A. pricei extracts on survival or growth, KB cells were exposed to 5, 10 or 20 μg/ml doses of desmethoxyyangonin and cardamonin for 24 h and for flavokawain B for 24, 48 or 72 h. Fig. 1B–D shows that cardamonin and flavokawain B induced cell death (viability or growth) in a dose- and time-dependent manner, as determined by trypan blue exclusion. However, desmethoxyyangonin concentrations of 5–20 μg/ml did not affect the number of KB cells at 24 h (Fig. 1A). The concentrations of flavokawain B required for 50% inhibition of KB cell viability (IC$_{50}$) were approximately 30.0, 5.7 and 4.3 μg/ml for 24, 48 and 72 h, respectively (Fig. 1D). The effect of flavokawain B on human HGF cells was then investigated. At 24 h, flavokawain B concentrations of 5, 10 and 20 μg/ml did not affect the number of HGF cells; however, flavokawain B concentrations of 30 and 40 μg/ml proved to be cytotoxic ($P<.05$) (Fig. 1E). Comparative experiments on the responses of KB and HGF cells to treatment with flavokawain B showed reduced cell viability in response to treatment in both cell lines, but the reduction was more pronounced in KB cells than in HGF cells.

3.2. Induction of apoptotic DNA fragmentation by flavokawain B

After incubation for 24 h, the majority of KB cells ($P<.05$) treated with flavokawain B (at 0, 5, 10 and 20 μg/ml) contained condensed nuclei (data not shown). Fig. 2 showed characteristic populations of flavokawain B-treated KB cells obtained using the TUNEL assay for DNA apoptotic fragmentation. Apoptotic cells were identified by their dark nuclei as seen under a light microscope.
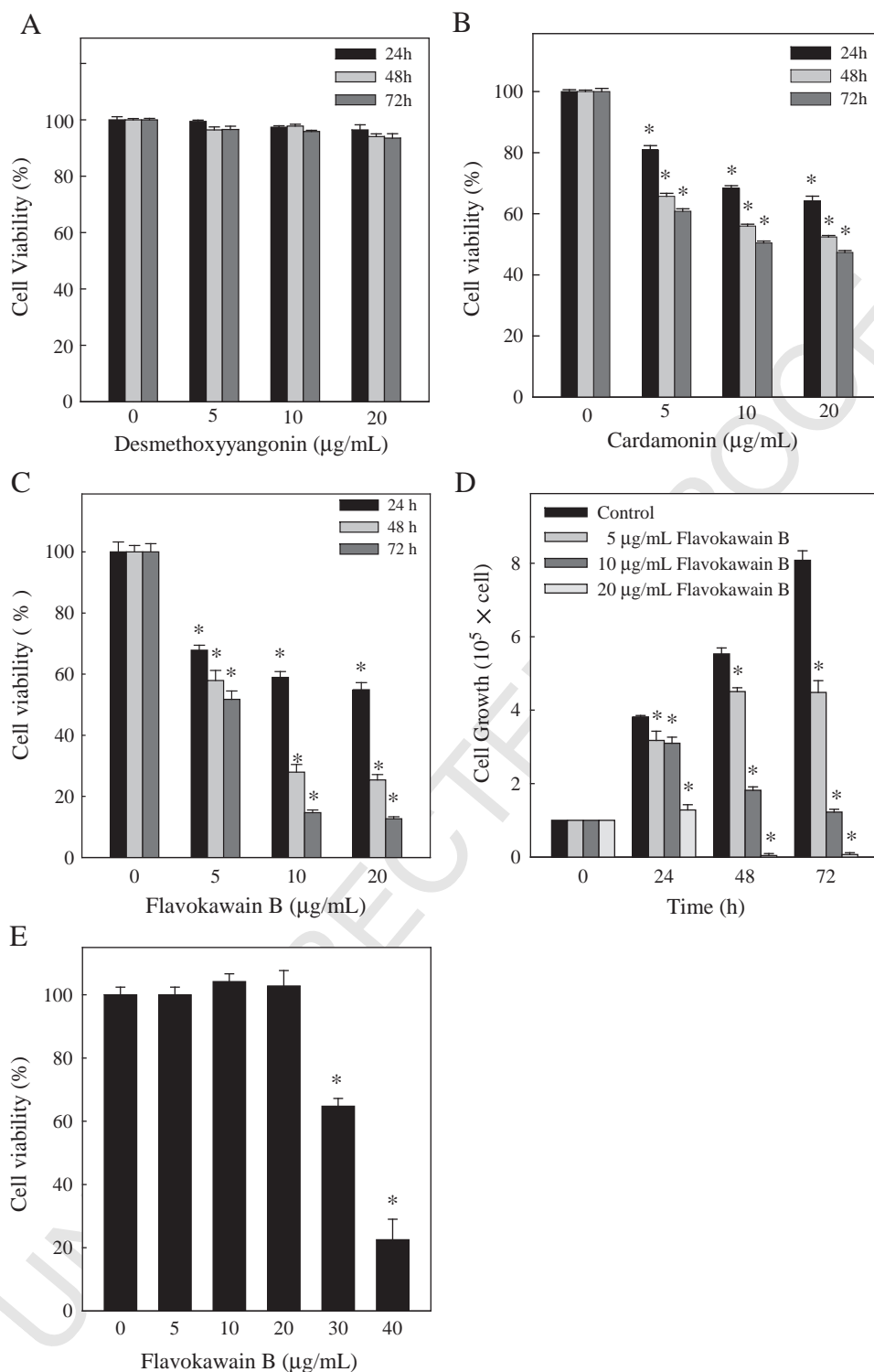
Fig. 1. Effects of desmethoxyyangonin, cardamonin and flavokawain B upon cell death (viability or growth) of human squamous carcinoma KB cells and normal HGF cells. (A–D) KB cells were treated with 0, 5, 10 or 20 μg/ml of (A) desmethoxyyangonin or (B) cardamonin for 24 h and (C and D) flavokawain B for 24, 48 or 72 h. Cultures were harvested and cell number determined by counting cell suspensions using a hemocytometer. (E) HGF cells were treated with 0, 5, 10, 20, 30 or 40 μg/ml of flavokawain B for 24 h. Cell numbers determined by counting cell suspensions using a hemocytometer. Results are presented as mean±S.D. of three assays. An asterisk (*) indicates a significant difference in comparison with the control group (P<.05).

328   *3.3. Sub-G1 accumulation and G2/M arrest in flavokawain B-treated*
329   *KB cells*

330   DNA content profiles of flavokawain B-treated KB cells were
331   obtained using flow cytometry to measure the fluorescence of PI–

DNA binding. Cells with less DNA staining relative to diploid analogs 332
were considered apoptotic. There was a remarkable (P<.05) accu- 333
mulation of subploid cells, the so-called sub-G1 peak, in flavokawain 334
B-treated KB cells (5–20 μg/ml for 24 h) compared with the untreated 335
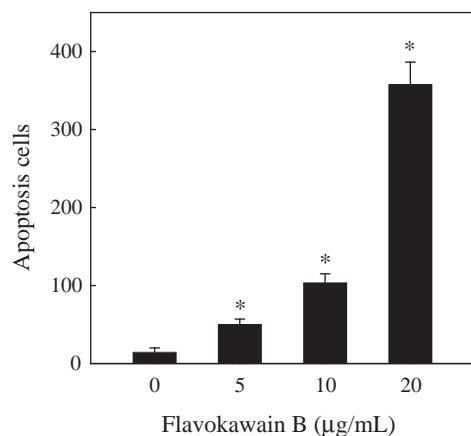group (Fig. 3). Furthermore, flavokawain B-induced growth 336

Fig. 2. TUNEL assay of KB cells exposed to flavokawain B. Cells treated with 0, 5, 10 or 20 μg/ml of flavokawain B for 24 h were examined under a light microscope (×400 magnification). The average number of apoptotic-positive cells in microscopic fields from three separate samples. An asterisk (*) indicates a significant difference in comparison with the control group ($P<.05$).

inhibition led to increased percentages of KB cells in G2/M and S phase, resulting in a progressive and sustained accumulation of cells in the G2/M phase. Correspondingly, percentages of cells in G1 phase decreased over time.

3.4. ROS generation and mitochondrial dysfunction in flavokawain B-treated KB cells

Fluorescence microscopic or flow cytometric analysis using DCFH-DA as a fluorescence probe was used for estimating the generation of ROS. Basal DCFH-DA fluorescence was demonstrated in the untreated KB cells (control). Incubation of cells with flavokawain B (10 μg/ml for 0, 1, 2 or 3 h) caused a significant increase in fluorescence, with a maximum ROS increase ($P<.05$) observed at 2 h after treatment (Fig. 4A). Dose-dependent increase ($P<.05$) in ROS generation after flavokawain B treatment (0, 5, 10 or 20 μg/ml for 2 h) were also observed (Fig. 4B). To determine whether an early loss of mitochondrial membrane potential occurred during treatment with flavokawain B, KB cells were grown in the absence (control) or in the presence of flavokawain B (10 μg/ml for 0, 1, 3 or 6 h). The mitochondrial membrane potential was determined by flow cytometry. Fig. 4C shows that treatment with flavokawain B resulted in loss of the mitochondrial membrane potential in KB cells ($P<.05$), indicating its ability to induce mitochondrial dysfunction.

(μg/mL)	Apoptotic cells	Non-apoptotic cells		
	sub-G1	G1	S	G2/M
0	0.3 ± 0.1	77.8 ± 1.2	13.0 ± 1.0	9.2 ± 0.2
5	1.0 ± 0.8*	59.8 ± 2.2*	16.8 ± 0.9*	23.5 ± 2.4*
10	6.8 ± 0.6*	56.1 ± 0.4*	20.7 ± 0.7*	23.9 ± 0.7*
20	16.6 ± 2.2*	55.2 ± 3.9*	22.8 ± 5.8*	22.0 ± 2.3*

Fig. 3. Effects of flavokawain B on cell cycle distribution in KB cells. Cells were treated with 0, 5, 10 or 20 μg/mll flavokawain B for 24 h, stained with PI and analyzed for sub-G1 and cell cycle phase using flow cytometry. Cellular distribution (percentage) in different phases of the cell cycle (sub-G1, G1, S and G2/M) after treatment with flavokawain B. Apoptotic nuclei were identified as a subploid DNA peak and distinguished from cell debris on the basis of forward light scattering and PI fluorescence. Results are presented as mean±S.D. of three assays. An asterisk (*) indicates a significant difference in comparison with the control group ($P<.05$).
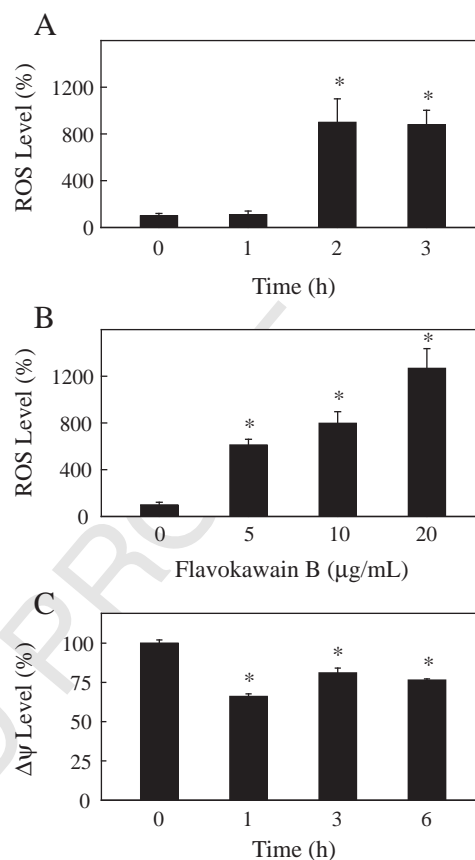

Fig. 4. Effects of flavokawain B on intracellular ROS levels and mitochondrial membrane potential in KB cells. (A and B) Cells were treated with 0–20 μg/ml of flavokawain B for 0, 1, 2 or 3 h. The nonfluorescent cell membrane-permeable probe DCFH-DA was added to the culture medium at a final concentration of 10 μmol/l 30 min before the end of each experiment. DCFH-DA was used to penetrate cells, react with cellular esterases and ROS and be metabolized into fluorescent DCF. The intracellular ROS level (as a percentage of the control), as indicated by DCF fluorescence, was measured by fluorescence microscopy (×200 magnification) (A and B). (C) Effect of flavokawain B on the mitochondrial membrane potential of KB cells. Cells were grown in the absence (control) or presence of flavokawain B (10 μg/ml) for 0, 1, 3 or 6 h; stained with DiOC6 and analyzed by flow cytometry as described in "Materials and Methods." The mitochondrial membrane potential after treatment with flavokawain B as a percentage of the control, as indicated by DiOC6 fluorescence, is shown. Results are the mean±S.D. of three assays. An asterisk (*) indicates a significant difference in comparison with the control group ($P<.05$).

3.5. Flavokawain B induces release of cytochrome c, activation of caspase-3 and -9 and cleavage of PARP

It has been reported that treatment of cells with a variety of chemotherapeutic agents is accompanied by increased cytosolic translocation of cytochrome c, activation of caspase-3 and degradation of PARP [17]. In the present study, cytosolic and mitochondrial levels of cytochrome c were examined using Western blot analysis. The results revealed that flavokawain B induced the release of cytosolic cytochrome c from 24 h after treatment (Fig. 5A). As cytochrome c is reportedly involved in the activation of the caspases that trigger apoptosis [17], we investigated the roles of caspase-3 and -9 in the cellular response to flavokawain B. Immunoblotting analysis revealed that treatment of KB cells with flavokawain B induced proteolytic cleavage of pro-caspase-3 and -9 into their active forms (Fig. 5A). Fig. 5A shows the increase in levels of cleaved caspase-9, and there seems to be no change in total pro-caspase-9 levels. Since PARP-specific proteolytic cleavage by caspase-3 is considered to be a biochemical characteristic of apoptosis, a Western blot experiment

was done using an antibody against PARP, a nuclear enzyme involved in DNA repair [18]. Fig. 5A demonstrates that following the addition of flavokawain B, the 115-kd PARP protein is cleaved to a 85-kd fragment in KB cells.

3.6. Activation of the Fas-mediated apoptosis pathway by flavokawain B results in activation of caspase-8 and cleavage of Bid

To assess whether flavokawain B (5–20 μg/ml for 24 h) promoted apoptosis via a receptor-mediated pathway, the levels of Fas and FasL proteins in KB cells were determined by Western blot. The results show that flavokawain B stimulated the expression of Fas and FasL (Fig. 5A). To verify whether the activation of caspase-8 is associated with Fas and FasL production in response to treatment with flavokawain B [19], involvement of caspase-8 activation is further supported by immuno-blotting analysis, with the results suggesting tat proteolytic cleavage of pro-caspase-8 is induced (Fig. 5A). Next, the expression levels of proapoptosis protein Bid, which produces the truncated Bid fragment upon cleavage by caspase-8, were measured. Bid fragment causes mitochondrial damage and amplifies apoptotic signals by activating the mitochondrial pathway [20]. The results indicate that flavokawain B induced down-regulation of Bid in KB cells (Fig. 5A).

3.7. Flavokawain B induces dysregulation of Bcl-2 and Bax proteins

As shown in Fig. 5B, incubation of KB cells with flavokawain B caused a dramatic reduction in the level of Bcl-2, a potent cell-death inhibitor, and increased the level of Bax protein, which hetero-dimerizes with and thereby inhibits Bcl-2. These results indicate that flavokawain B induced dysregulation of Bcl-2 and Bax in KB cells.

3.8. Inhibitory effects of flavokawain B on cyclin A, cyclin B1, Cdc2 and Cdc25C expression

In order to examine the molecular mechanism(s) and underlying changes in cell cycle patterns caused by flavokawain B treatment, we investigated the effects upon various cyclins and CDKs involved in cell cycle control in KB cells. KB cells were treated with flavokawain B (5–20 μg/ml) for 24 h. Dose- and time-dependent reductions in mitotic cyclins A and B1, mitotic-cyclin-dependent kinase Cdc2 and mitotic phosphatase Cdc25C expression were observed (Fig. 6A). These results imply that flavokawain B inhibits cell cycle progression by reducing levels of cyclin A, cyclin B1, Cdc2 and Cdc25C.

3.9. Flavokawain B increases the expression of p21/WAF1, Wee1 and p53

As shown in this study, treatment of KB cells with flavokawain B resulted in cell cycle arrest. The effect of exposure to flavokawain B on cell cycle-regulatory molecules, including p21/WAF1 (CDK inhibitors), Wee1 (CDK relative factors) and p53, was then examined. Fig. 6A shows that treatment of KB cells with flavokawain B (5–20 μg/ml for 24 h) induced marked ($P<.05$) dose- and time-dependent up-regulation of p21/WAF1, Wee1 and p53 protein expression.
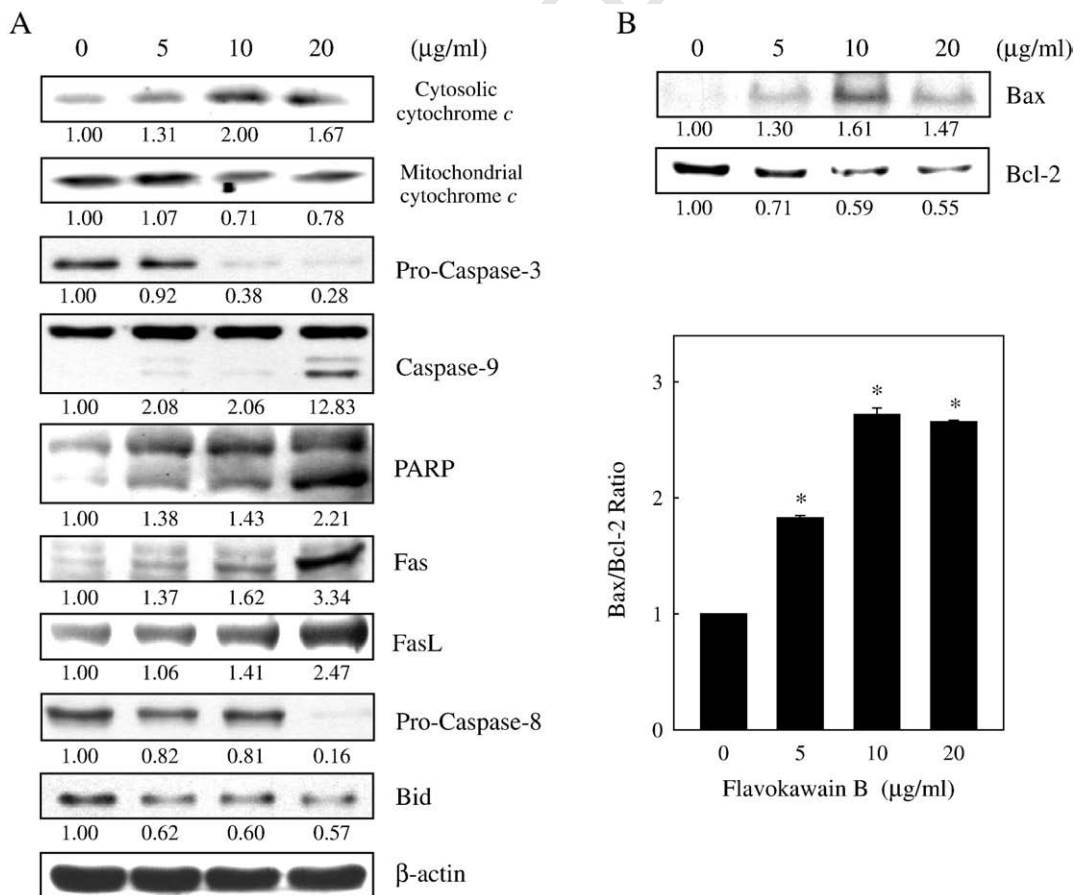

Fig. 5. Western blot analysis of mitochondrial and cytosolic cytochrome *c*, caspase-3, caspase-8, caspase-9, PARP, Fas, FasL, Bid (A) and Bcl-2 and Bax protein levels (B) in KB cells exposed to flavokawain B. Cells were treated with 0, 5, 10 or 20 μg/ml flavokawain B for 24 h. Protein (50 μg) from each sample was resolved by SDS-PAGE (8%–15% polyacrylamide gel) with β-actin as a control. Relative changes in protein bands were measured by densitometry. A typical result from three independent experiments is shown.
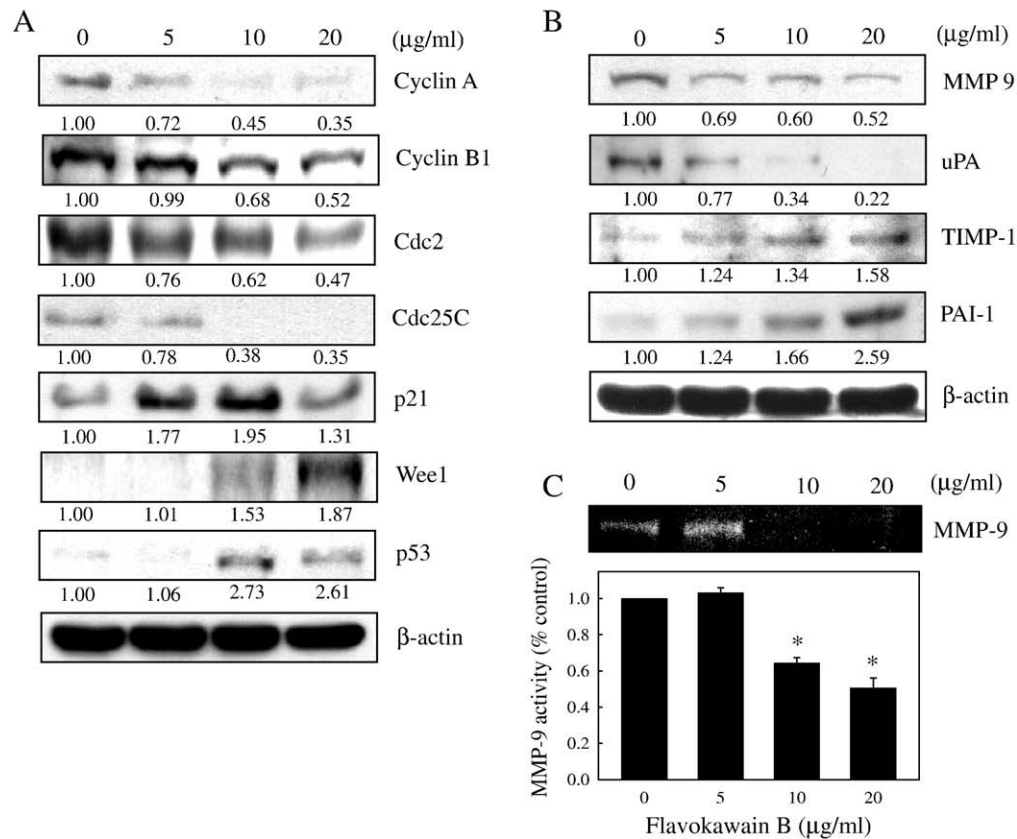
Fig. 6. Western blot analysis of cyclin A, cyclin B1, Cdc2, Cdc25C, p21/WAF1, Wee1, p53 (A), MMP-9, u-PA, TIMP-1 and PAI-1 protein levels (B) and MMP-9 activity (C) in KB cells after exposure to flavokawain B. (A and B) Cells were treated with 0, 5, 10 or 20 μg/ml flavokawain B for 24 h. Protein (50 μg) from each sample was resolved by SDS-PAGE (8%–15% polyacrylamide gel) and Western blot analysis with β-actin as a control. (C) Cells were treated with 0, 5, 10 or 20 μg/ml flavokawain B for 24 h and then subjected to gelatin zymography to analyze MMP-9 activity. Relative changes in bands were measured by densitometry. Typical results from three independent experiments are shown. Results are presented as mean±S.D. of three assays. An asterisk (*) indicates a significant difference in comparison with the control group ($P<.05$).

3.10. Effects of flavokawain B on levels of MMP-9, u-PA, TIMP-1 and PAI-1 and on activity of MMP-9

Western blotting was used to analyze the effects of flavokawain B on the expression of the metastasis-related proteins MMP-9, u-PA, TIMP-1 and PAI-1. As shown in Fig. 6B, treatment of KB cells with flavokawain B (5–20 μg/ml for 24 h) markedly ($P<.05$) induced dose-dependent reduction of the expression levels of MMP-9 and u-PA. Dose-dependent up-regulation of the expression of their specific endogenous inhibitors, TIMP-1 and PAI-1, was found after treatment with flavokawain B (Fig. 6B). Moreover, gelatin zymography assays showed that flavokawain B (5–20 μg/ml for 24 h) reduced MMP-9 activity in a dose-dependent manner in KB cells (Fig. 6C).

3.11. In vivo inhibition of KB xenograft growth by flavokawain B

Nude mice were used to evaluate the in vivo effects of flavokawain B on tumor growth. KB cells were xenografted into nude mice as described in "Materials and Methods." All animals appeared healthy, with no loss of body weight noted during flavokawain B treatment (Fig. 7A). In addition, no signs of toxicity were observed in any of the nude mice (body weight and microscopic examination of individual organs; data not shown). The time course for KB xenograft growth with flavokawain B (0.75 mg/kg every 2 days) or with vehicle only (control) is shown in Fig. 7B. Evaluation of tumor volume showed significant time-dependent growth inhibition associated with flavokawain B treatment. Tumor volume in the flavokawain B-treated mice was inhibited compared with the control group (Fig. 7C). At the end of 27 days, the KB xenograft tumor was excised from each animal that was killed. In addition, microscopic examination of tumor sections was done to distinguish differences in nucleic and cytoplasmic morphology after 27 days of flavokawain B treatment. As shown in Fig. 8A, the histopathological findings from inoculated squamous cell carcinomas in tumor control nude mice presented newly formed blood vessels with massive necrosis in the area of the tumor mass. Tumor cells were large, round to oval in shape with predominant nucleoli and expressed high levels of cellular activity and mitotic figures. In contrast, tumors in the flavokawain B-treated nude mice showed less angiogenesis, had smaller cells with shrunken and had condensed and pyknotic nuclei, indicating tumor cell inactivity or regression (Fig. 8A). Interestingly, while abundant mitosis was observed in the proliferating cells in the control group, few mitotic cells were seen in sections from flavokawain B-treated animals (Fig. 8B). These results demonstrate flavokawain B-related antitumor activity in nude mice bearing KB epidermoid carcinoma xenografts.

3.12. Induction of apoptotic DNA fragmentation by flavokawain B in xenograft tumors

The effect of flavokawain B on tumor growth (apoptosis) in the KB xenograft mice was also examined using the TUNEL assay on tumor sections. Fig. 9A, B shows that there were more TUNEL-positive cells in tumors from flavokawain B-treated animals, compared to untreated controls ($P<.05$), which demonstrates that flavokawain B treatment was associated with decreased proliferation and increased apoptosis in the study animals. Analysis of our data suggests that
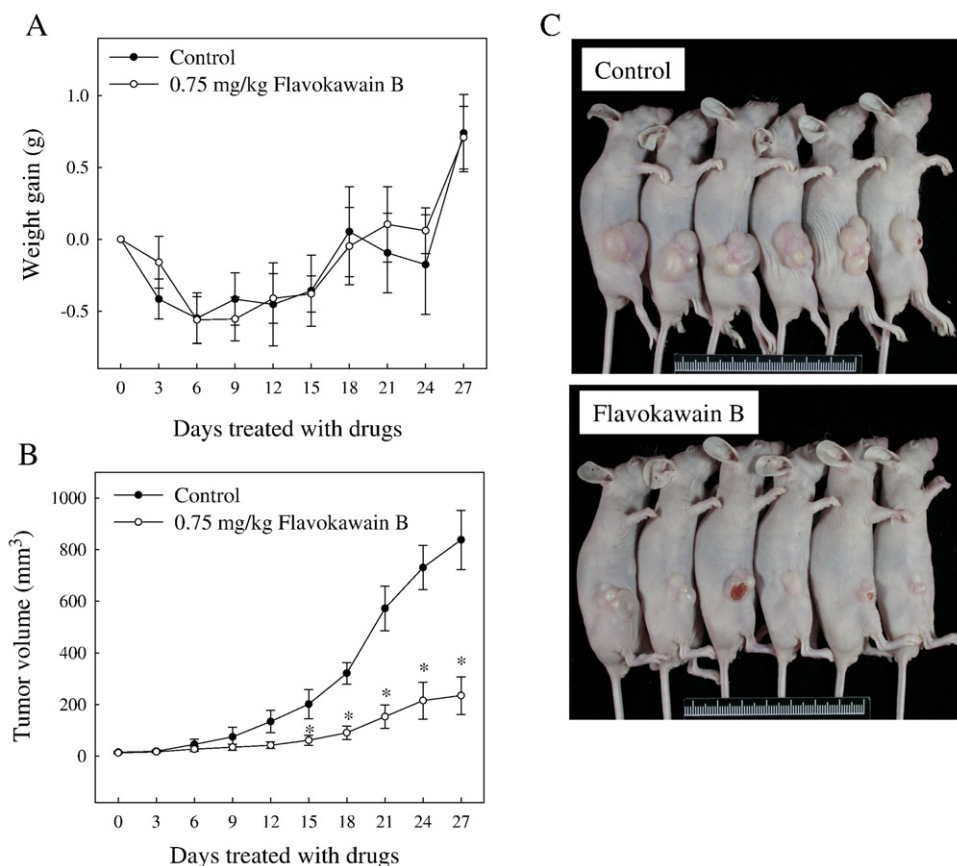
Fig. 7. *In vivo* inhibition of KB xenograft proliferation by flavokawain B. Time-course effect of flavokawain B on growth of KB xenografted nude mice was evaluated by measurements of body weight (A) and tumor volume (B) every 3 days. KB cells were implanted subcutaneously into the flanks of nude mice on day 0, and animals were subsequently treated with 0.75 mg/kg of flavokawain B or vehicle only (control). (C) On the 27th day after tumor implantation, animals were photographed. Results are presented as mean±S.E. (*n*=6). An asterisk (*) indicates a significant difference in comparison with control group (*P*<.05).

flavokawain B promoted antitumor activity in nude mice bearing KB epidermoid carcinoma xenografts.

4. Discussion

This study documents the chemopreventive effects of flavokawain B, a chalcone purified from *A. pricei*, *in vitro* cell culture and *in vivo* nude mice models of human squamous carcinoma KB cells. Chalcones form an important class of naturally occurring biological compounds with a widespread distribution in fruits, vegetables, spices, tea and soy-based foodstuffs and have been the subject of great interest for their biological activities [9]. In structure, chalcones are open-chain flavonoids in which the two aromatic rings are joined by a three-carbon α, β-unsaturated carbonyl system. A vast number of naturally occurring chalcones are polyhydroxylated on the aryl rings. The radical-quenching properties of the phenolic groups present in many chalcones have raised interest in using these compounds or chalcone-rich plant extracts as food preservatives [10]. We showed that flavokawain B, a chalcone derivative, directly inhibited cell viability and growth of KB cells by induction of cell cycle arrest and apoptosis. Interestingly, flavokawain B has been found to show less cytotoxicity in normal HGF cells. Furthermore, *in vivo* tumor inhibition by flavokawain B was observed in the nude mice xenograft model in this study. Both incidence and mean tumor volume were significantly reduced by flavokawain B treatment. Immunohisto-chemical staining revealed increased apoptosis (TUNEL assay) in tumors from flavokawain B-treated animals. Analysis of our data suggests that flavokawain B could inhibit proliferation of human squamous carcinoma KB cells both *in vitro* and *in vivo*. The chemopreventive properties of flavokawain B combined with the epidemiologic and experimental data [11,12] prompted this study into the inhibitory effects of treatment with flavokawain B upon human squamous carcinoma cells.

Apoptosis is an important homeostatic mechanism that balances cell division and cell death and maintains the appropriate number of cells in the body. Many studies have shown associations between apoptosis and cancer, and apoptosis-inducing agents are being investigated as tools for the management of cancer. Apoptosis is controlled by two major pathways; a mitochondrial pathway [17] and a membrane death receptor (DR) pathway [19]. The first involves the participation of mitochondria and, in most forms of apoptosis, is a response to cellular stress, loss of survival factors and developmental cues [17]. The second pathway involves the interaction of cell surface receptors, such as Fas, TNFR, DR3, DR4 and DR5, with their ligands. In the former, activation of DRs (Fas) by cross-linking with their natural ligands (FasL) leads to receptor clustering and formation of a death-inducing signaling complex, which results in the activation of pro-caspase-8, which subsequently promotes proteolytic processing of pro-caspase-3 and Bid [19]. In the latter, the loss of mitochondrial membrane potential induces the release of cytochrome *c* from mitochondria into the cytosol, where it binds to apoptotic protease activation factor-1. Meanwhile, pro-caspase-9 also binds to apoptotic protease activation factor-1, and
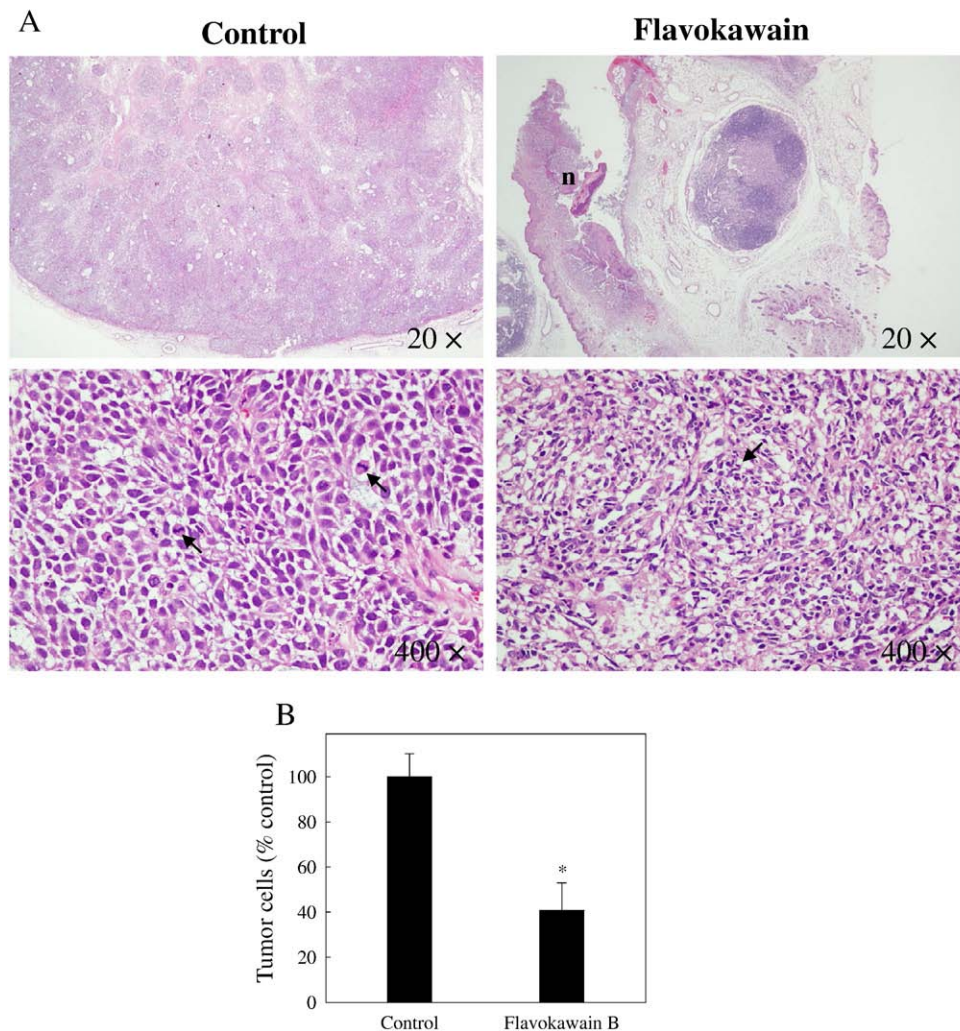
Fig. 8. Histochemical analysis of proliferation in KB xenograft tumors. (A) Control KB xenograft tumors and KB xenograft tumors following flavokawain B (0.75 mg/kg) treatment were examined using a light microscopy. Arrows indicate mitotic (tumor control) and pyknotic tumor cells (flavokawain B). Typical results from three independent experiments are shown. (B) Percentages of living cells in microscopic fields ($\times$400 magnification) from six tumor samples were quantified and expressed compared with tumor control (100%). An asterisk (*) indicates a significant difference in comparison with the control group ($P<.05$).

this interaction activates pro-caspase-9. Activated caspase-9 activates downstream pro-caspase-3 [17,18]. Activated caspase-3 is responsible for the proteolytic degradation of PARP, which occurs at the onset of apoptosis [18]. The present study demonstrates that treatment of KB cells with flavokawain B can induce apoptotic cell death associated with internucleosomal DNA fragmentation; sub-G1 phase accumulation; elevation of ROS; loss of mitochondrial membrane potential; translocation of cytochrome c; activation of caspase-3, -8 and -9; degradation of PARP; dysregulation of Bcl-2 and Bax; induction of Fas and FasL expression and down-regulation of Bid. Data from the present study suggest that flavokawain B-induced apoptosis is controlled by both mitochondrial and membrane DR pathways.

It has been shown that the Bcl-2 family of proteins has an important regulatory role in apoptosis, both in activation (Bax) and inhibition (Bcl-2) [21]. Of the Bcl-2 family members, the Bcl-2/Bax protein ratio has been recognized as a key factor in regulation of the apoptotic process [21]. In the present study, the increase in flavokawain B-induced apoptosis was associated with a reduction in the levels of Bcl-2, a potent cell-death inhibitor, as well as an increase in the levels of Bax protein, which heterodimerizes with,

and thereby inhibits, Bcl-2. These data indicate that flavokawain B treatment disturbs the Bcl-2/Bax ratio and thereby leads to apoptosis of KB cells.

Many of the agents that induce apoptosis are oxidants or stimulators of cellular oxidative metabolism, while many inhibitors of apoptosis show antioxidant activity. Indeed, factors that cause or promote oxidative stress, such as ROS production, lipid peroxidation, down-regulation of antioxidant defences characterized by reduced glutathione levels and reduced transcription of superoxide dismutase, catalase and thioredoxin, have been shown to be involved in some apoptotic processes [22,23]. Moreover, ROS can play an important role in apoptosis by regulating the activity of certain enzymes involved in the cell-death pathway [22,23]. All of these factors point to a significant role for intracellular oxidative metabolites in the regulation of apoptosis. Earlier studies have shown that many stimuli such as anticancer drugs can cause cells to produce ROS, which mediate mitochondria-initiated apoptosis by inducing the loss of mitochondrial membrane potential [24]. In this study, we also observed that flavokawain B significantly inhibits KB cell survival concomitant with partial augmentation of ROS accumulation, which is playing major role in apoptosis. However,
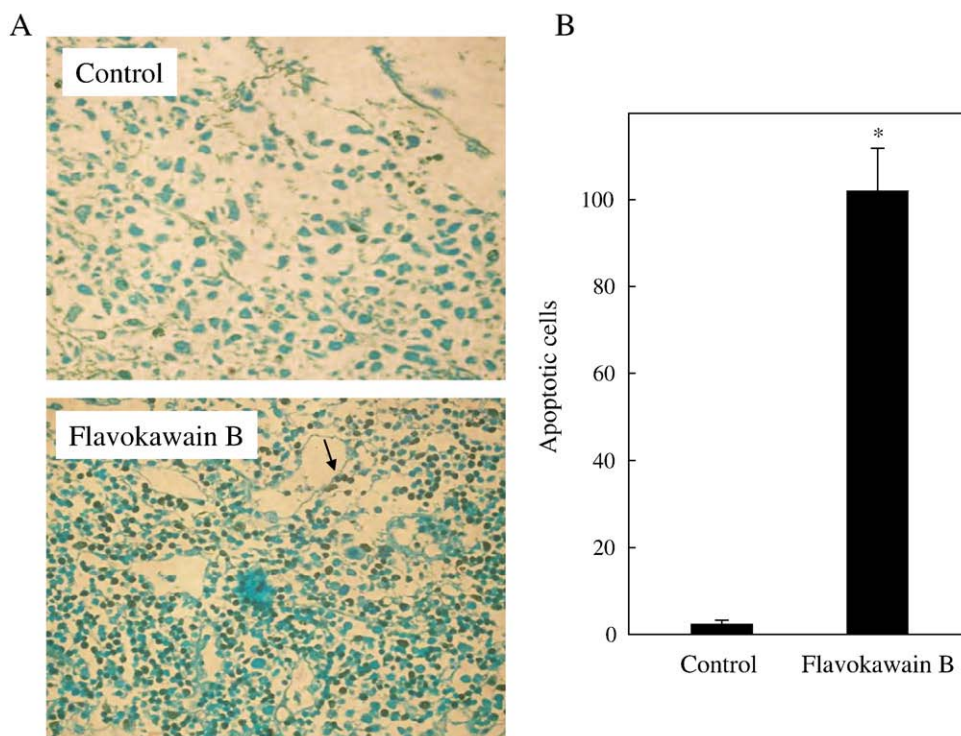
Fig. 9. Immunohistochemical staining of apoptotic DNA fragmentation in KB xenograft tumors. (A) *In situ* apoptosis detection using TUNEL staining in tumor sections from control animals and experimental analogs treated with flavokawain B (0.75 mg/kg). Arrow indicates example apoptotic-positive cells (×400 magnification). Typical results from three independent experiments are shown. (B) The number of apoptotic-positive cells in microscopic fields from three samples was averaged. An asterisk (*) indicates a significant difference in comparison with the control group (*P*<.05).

further investigations warranted to confirm flavokawain B-induced ROS generation in KB cells.

Disturbance of the cancer cell cycle is one of the therapeutic targets for development of new anticancer agents. The results of cell cycle analysis in the present study, as evaluated by flow cytometry, show that treatment with flavokawain B had a profound effect on cell cycle control, with squamous carcinoma cells accumulating in the G2/M phase. This cell cycle blockade was associated with reductions in cyclin A, cyclin B1, Cdc2 and Cdc25C and increased CDK inhibitor p21/WAF1, Wee1 and p53. Eukaryotic cell cycle progression involves the sequential activation of CDKs, whose activation is dependent on association with cyclins. Among CDKs that regulate cell cycle progression, CDK2 and Cdc2 kinases are activated primarily in association with cyclin A and cyclin B1 during progression of the G2/M phase [25]. The phosphorylation of Tyr15 of Cdc2 suppresses activity of the Cdc2/cyclin A and B1 kinase complex. Dephosphorylation of Tyr15 of Cdc2 is catalyzed by Cdc25C phosphatase, and this reaction is believed to be the rate-limiting step for entry into mitosis [26]. Cell cycle progression is also regulated by the relative balance between the cellular concentrations of CDK inhibitors such as p21/WAF1, which may help to maintain G2/M cell cycle arrest by inactivating the cyclin B1/Cdc2 complex, disrupting the interaction between proliferating cell nuclear antigen and Cdc25C [27]. Wee1 protein kinase negatively regulates entry into mitosis by catalyzing the inhibitory tyrosine phosphorylation of Cdc2-cyclin B kinase [28]. p53 could act as a sensor for DNA damage that arrests the cell cycle for DNA repair or up-regulates proapoptotic factors, resulting in increased susceptibility to apoptosis [27]. The results imply that the expression levels of cyclin A, cyclin B, Cdc2 and Cdc25C are down-regulated and that p21/WAF1, Wee1 and p53 levels are increased in flavokawain B-treated KB cells, which is consistent with a G2/M block. Analysis of our data suggests that the observed inhibition of KB cell growth associated with flavokawain B treatment could be the result of cell cycle arrest during the G2/M phase.

There is increasing evidence that the related processes of neoplastic transformation, progression and metastasis involve alteration of the normal apoptotic pathways. In this study, we reveal that flavokawain B extracts decreased the levels of tumor metastasis-related proteins, such as MMP-9 and u-PA, in KB cells. Meanwhile, their endogenous inhibitors TIMP-1 and PAI-1 were increased in KB cells. Metastasis is the spread of cancer cells from the primary tumor to new metastatic sites via the blood or lymph vessels [29]. MMPs and u-PA, which are secreted by invasive cancer cells, have important roles in cancer cell invasion and metastasis because tumor cells must cross the type IV collagen-rich basement membrane of vessel walls to spread to other sites during cancer metastasis [14]. Therefore, inhibition of invasion mediated by MMPs and u-PA may be a key feature of treatments that can successfully prevent cancer metastasis. The physiological activity of MMPs and u-PA was highly correlated to their specific endogenous inhibitors TIMPs and PAIs, respectively. TIMPs has a key role in determining the proteolytic activity of tumor tissues by regulating the activity of MMPs. PAIs (serine protease inhibitors) regulate u-PA and the tissue plasminogen activator (tPA) to control plasmin generation. TIMPs and PAIs have been implicated as mediators of invasion and metastasis in several types of tumor [30,31]. It has been shown that KB cells exhibit reduced motility and reflect fewer invasions without altering the MMP status [32]. Therefore, the inhibition of KB cell migration and invasion by flavokawain B was not examined in this study.

The results obtained *in vitro* and *in vivo* in this study imply that flavokawain B could act as a chemopreventive agent with respect to inhibition of the growth of human squamous carcinoma KB cells through the induction of cell cycle arrest and apoptosis. These data provide an important step that might help model the effects of

flavokawain B for potential future studies with animal models and human patients and thereby facilitate the development of nutraceutical products using this agent.

Acknowledgments

References

[1] Larsen K, Ibrahim H, Khaw SH, Saw LG. In: Wong KM, editor. ~~Natural history publications, Borneo. Gingers of Peninsular Malaysia and Singapore; 1999. p. 135. Kota Kinabalu, Sabah~~.
[2] Yang HL, Chen SC, Chen CS, Wang SY, Hseu YC. *Alpinia pricei* rhizome extracts induce apoptosis of human carcinoma KB cells via a mitochondria-dependent apoptotic pathway. Food Chem Toxicol 2008;46:3318–24.
[3] Lin CT, Kumar KJS, Tseng YH, Wang ZJ, Pan MY, Xiao JH. Anti-inflammatory activity of flavokawain B from *Alpinia pricei* Hayata. J Agric Food Chem 2009;57:6060–5.
[4] Chen IN, Chang CC, Ng CC, Wang CY, Shyu YT, Chang TL. Antioxidant and antimicrobial activity of Zingiberaceae plants in Taiwan. Plant Foods Hum Nutr 2008;63:15–20.
[5] Hseu YC, Chen CS, Wang SY. *Alpinia pricei rhizome extracts* induce cell cycle arrest in human squamous carcinoma KB cells and suppress tumor growth in nude mice. Evid Based Complement Alternat Med ~~2009 (accepted)~~.
[6] Evan GI, Vousden KH. Proliferation, cell cycle and apoptosis in cancer. Nature 2001;411:342–8.
[7] Sherr CJ. The ins and outs of RB: coupling gene expression to the cell cycle clock. Trends Cell Biol 1994;4:15–8.
[8] Wyllie AH. Apoptosis: cell death in tissue regulation. J Pathol 1987;153:313–6.
[9] Go ML, Wu X, Liu XL. Chalcones: an update on cytotoxic and chemoprotective properties. Curr Med Chem 2005;12:481–99.
[10] Dhar DN. The chemistry of chalcones and related compounds. New York: John Wiley; 1981.
[11] Zi X, Simoneau AR. Flavokawain A, a novel chalcone from kava extract, induces apoptosis in bladder cancer cells by involvement of Bax protein-dependent and mitochondria-dependent apoptotic pathway and suppresses tumor growth in mice. Cancer Res 2005;65:3479–86.
[12] Steiner GG. The correlation between cancer incidence and kava consumption. Hawaii Med J 2000;59:420–2.
[13] Masters JR. HeLa cells 50 years on: the good, the bad and the ugly. Nat Rev Cancer 2002;2:315–9.
[14] Westermarck J, Kahari VM. Regulation of matrix metalloproteinase expression in tumor invasion. FASEB J 1999;13:781–92.
[15] Collins A, Yuan L, Kiefer TL, Cheng Q, Lai L, Hill SM. Overexpression of the MT1 melatonin receptor in MCF-7 human breast cancer cells inhibits mammary tumor formation in nude mice. Cancer Lett 2003;89:49–57.
[16] Gavrieli Y, Sherman Y, Ben-Sasson SA. Identification of programmed cell death in situ via specific labeling of nuclear DNA fragmentation. J Cell Biol 1992;119:493–501.
[17] Green DR, Reed JC. Mitochondria and apoptosis. Science 1998;281:1309–12.
[18] Tewari M, Quan LT, O'Rourke K, Desnoyers S, Zeng Z, Beidler DR. Yama/CPP32 beta, a mammalian homolog of CED-3, is a CrmA-inhibitable protease that cleaves the death substrate poly(ADP-ribose) polymerase. Cell 1995;81:801–9.
[19] Ashkenazi A, Dixit VM. Apoptosis control by death and decoy receptors. Curr Opin Cell Biol 1999;11:255–60.
[20] Eskes R, Desagher S, Antonsson B, Martinou JC. Bid induces the oligomerization and insertion of Bax into the outer mitochondrial membrane. Mol Cell Biol 2000;20:929–35.
[21] Adams JM, Cory S. The Bcl-2 protein family: arbiters of cell survival. Science 1998;281:1322–6.
[22] Briehl MM, Baker AF. Modulation of the antioxidant defense as a factor in apoptosis. Cell Death Differ 1996;3:63–70.
[23] Marchetti P, Castedo M, Susin SA, Zamzami N, Hirsch T, Macho A. Mitochondrial permeability transition is a central coordinating event of apoptosis. J Exp Med 1996;184:1155–60.
[24] Zhuge J, Cederbaum AI. Serum deprivation-induced HepG2 cell death is potentiated by CYP2E1. Free Radic Biol Med 2006;40:63–74.
[25] Stark GR, Taylor WR. Analyzing the G2/M checkpoint. Methods Mol Cell Biol 2004;280:51–82.
[26] Bulavin DV, Higashimoto Y, Demidenko ZN, Meek S, Graves P, Phillips C, et al. Dual phosphorylation controls Cdc25 phosphatases and mitotic entry. Nat Cell Biol 2003;5:545–51.
[27] Guillot C, Falette N, Paperin MP, Courtois S, Gentil-Perret A, Treilleux I, et al. p21WAF1/CIP response to genotoxic agents in wild type TP53 expression breast primary tumors. Oncogene 1997;14:45–52.
[28] Parker LL, Piwnica-Worms H. Inactivation of the p34cdc2-cyclin B complex by the human WEE1 tyrosine kinase. Science 1992;257:1955–7.
[29] Stacker SA, Baldwin ME, Achen MG. The role of tumor lymph angiogenesis in metastatic spread. FASEB J 2002;16:922–34.
[30] Andreasen PA, Egelund R, Petersen HH. The plasminogen activation system in tumor growth, invasion, and metastasis. Cell Mol Life Sci 2000;57:25–40.
[31] Verstappen J, Von den Hoff JW. Tissue inhibitors of metalloproteinases (TIMPs): their biological functions and involvement in oral disease. J Dent Res 2006;85:1074–84.
[32] Khan MH, Yasuda M, Higashino F, Haque S, Kohgo T, Nakamura M, et al. nm23-H1 suppresses invasion of oral squamous cell carcinoma-derived cell lines without modifying matrix metalloproteinase-2 and matrix metalloproteinase-9 expression. Am J Pathol 2001;158:1785–91.

AUTHOR QUERY FORM

ELSEVIER	**Journal: JNB** **Article Number: 6665**	**Please e-mail or fax your responses and any corrections to:** **Jill Shepherd** **E-mail: J.Shepherd@Elsevier.com** **Tel: 352-483-8113** **Fax: 352-483-3417**

Dear Author,

Any queries or remarks that have arisen during the processing of your manuscript are listed below and highlighted by flags in the proof. Please check your proof carefully and mark all corrections at the appropriate place in the proof (e.g., by using on-screen annotation in the PDF file) or compile them in a separate list.

For correction or revision of any artwork, please consult http://www.elsevier.com/artworkinstructions.

Any queries or remarks that have arisen during the processing of your manuscript are listed below and highlighted by flags in the proof. Click on the 'Q' link to go to the location in the proof.

Location in article	Query / Remark: click on the Q link to go Please insert your reply or correction at the corresponding line in the proof
Q1	Please provide postal code for all affiliations.
Q2	Please replace PARP with its expanded form, if any.
Q3	Please provide the expanded form of PARP, if any.
Q4	Please expand TBS here.
Q5	Please expand PMSF here.
Q6	Please expand BSA here.
Q7	Please replace the expanded form of CBB, if any.
Q8	Please expand TBS here.
Q9	Please expand TNFR here.
Q10	Please provide publisher name here.
Q11	Please provide page-range here.

Thank you for your assistance.